

NEW TURBULENT SCALING LAWS FROM THE MULTI-POINT CORRELATION EQUATIONS

Andreas Rosteck¹ and Martin Oberlack^{1,2,3}

¹Chair of Fluid Dynamics, Dept. Mech. Eng., TU Darmstadt, Otto-Berndt-Str. 2, 64287 Darmstadt, Germany

²Center of Smart Interfaces, TU Darmstadt, Germany

³GS Computational Engineering, TU Darmstadt, Germany

oberlack@fdy.tu-darmstadt.de

ABSTRACT

In order to better understand and describe statistical quantities such as the mean velocity or higher order moments of turbulent flows, it is our aim to deduce scaling laws from the infinite hierarchy of multi-point correlation equations. The mathematical method employed will be the Lie-point symmetries. The method is rather generic and will be applied to different canonical flows, such as channel flows with and without rotation, where rotation about different axes are considered.

Equations of statistical turbulence theory

The velocity U and the normalized pressure P are decomposed according to the Reynolds decomposition, i.e. $U = \bar{U} + u$ and $P = \bar{P} + p$, where the overbar denotes averaged quantities and fluctuations are given by lower case letters. With this the Reynolds averaged Navier-Stokes equations write

$$\frac{\partial \bar{U}_i}{\partial t} + \bar{U}_k \frac{\partial \bar{U}_i}{\partial x_k} = - \frac{\partial \bar{P}}{\partial x_i} + \nu \frac{\partial^2 \bar{U}_i}{\partial x_k \partial x_k} - \frac{\partial \overline{u_i u_k}}{\partial x_k}, \quad i = 1, 2, 3,$$

where $t \in \mathbb{R}^+$ and $\mathbf{x} \in \mathbb{R}^3$ represent time and position vector. Viscosity $\nu > 0$ and density has been absorbed into the pressure.

In order to deal with the closure problem of turbulence, represented through the Reynolds stress tensor $\overline{u_i u_k}$ in our equations, we introduce the multi-point approach Keller & Friedmann (1925). Considering the infinite set of correlation equations has the advantage that the closure problem is somehow bypassed. Furthermore, the multi-point correlation (MPC) delivers additional information on the turbulence statistics such as length scale information which may not be gained from the Reynolds stress tensor, alone, which is a single-point approach.

Rather different to the classical approach of correlation functions, which is based on the fluctuating values of velocity and pressure, u_i and p , we presently first employ the instantaneous values U_i and P for the correlation as in this framework the finding of symmetries is considerably easier.

For this we first define

$$H_{i_{(n+1)}} = H_{i_{(0)}i_{(1)}\dots i_{(n)}} = \overline{U_{i_{(0)}}(\mathbf{x}_{(0)}, t) \dots U_{i_{(n)}}(\mathbf{x}_{(n)}, t)}, \quad (1)$$

where the index i of the farthestmost left quantity refers to its tensor character, while its superscript in curly brackets denotes the tensor order. The mean velocity is given by the first order tensor as $H_{i_{(1)}} = H_{i_{(0)}} = \bar{U}_i$. Using (1) and employing the Navier-Stokes equation we derive the MPC equation

$$\begin{aligned} \mathcal{F}_{i_{(n+1)}} = & \frac{\partial H_{i_{(n+1)}}}{\partial t} + \sum_{l=0}^n \left[\frac{\partial H_{i_{(n+2)}[i_{(n+1)} \mapsto k_{(l)}]}[\mathbf{x}_{(n+1)} \mapsto \mathbf{x}_{(l)}]}{\partial x_{k_{(l)}}} \right. \\ & \left. + \frac{\partial I_{i_{(n)}[l]}}{\partial x_{i_{(l)}}} - \nu \frac{\partial^2 H_{i_{(n+1)}}}{\partial x_{k_{(l)}} \partial x_{k_{(l)}}} \right] = 0 \text{ for } n = 1, \dots, \infty. \quad (2) \end{aligned}$$

where we need to further define

$$H_{i_{(n+2)}[i_{(n+1)} \mapsto k_{(l)}]}[\mathbf{x}_{(n+1)} \mapsto \mathbf{x}_{(l)}] = \overline{U_{i_{(0)}}(\mathbf{x}_{(0)}, t) \dots U_{i_{(n)}}(\mathbf{x}_{(n)}, t) U_{k_{(l)}}(\mathbf{x}_{(l)}, t)}, \quad (3)$$

and

$$I_{i_{(n)}[l]} = \overline{U_{i_{(0)}}(\mathbf{x}_{(0)}, t) \dots P(\mathbf{x}_{(l)}, t) \dots U_{i_{(n)}}(\mathbf{x}_{(n)}, t)}. \quad (4)$$

(2) may finally completed by continuity equations for all correlations (see e.g. Rosteck, 2013) which are not shown here. It is especially the linear form of the correlation equations (2) which made it possible to derive the sub-sequent symmetries.

Still, Reynolds decomposition and the resulting correlation functions based on the fluctuating quantities u and p may also be employed to derive a related MPC tensor

$$R_{i_{(n+1)}} = R_{i_{(0)}i_{(1)}\dots i_{(n)}} = \overline{u_{i_{(0)}}(\mathbf{x}_{(0)}) \dots u_{i_{(n)}}(\mathbf{x}_{(n)})}$$

and

$$P_{i_{(n)}[l]} = \overline{u_{i_{(0)}}(\mathbf{x}_{(0)}, t) \dots p(\mathbf{x}_{(l)}, t) \dots u_{i_{(n)}}(\mathbf{x}_{(n)}, t)}. \quad (5)$$

From the Navier-Stokes equations follows the transport equation of the MPC may be derived

$$\begin{aligned} \mathcal{F}_{i_{(n+1)}} = & \frac{\partial R_{i_{(n+1)}}}{\partial t} + \sum_{l=0}^n \left[\bar{U}_{k_{(l)}}(\mathbf{x}_{(l)}) \frac{\partial R_{i_{(n+1)}}}{\partial x_{k_{(l)}}} \right. \\ & + R_{i_{(n+1)}[i_{(l)} \mapsto k_{(l)}]} \frac{\partial \bar{U}_{i_{(l)}}(\mathbf{x}_{(l)})}{\partial x_{k_{(l)}}} + \frac{\partial P_{i_{(n)}[l]}}{\partial x_{i_{(l)}}} \\ & - \nu \frac{\partial^2 R_{i_{(n+1)}}}{\partial x_{k_{(l)}} \partial x_{k_{(l)}}} - R_{i_{(n)}[i_{(l)} \mapsto \emptyset]} \frac{\partial \overline{u_{i_{(l)}} u_{k_{(l)}}}(\mathbf{x}_{(l)})}{\partial x_{k_{(l)}}} \\ & \left. + \frac{\partial R_{i_{(n+2)}[i_{(n+1)} \mapsto k_{(l)}]}[\mathbf{x}_{(n+1)} \mapsto \mathbf{x}_{(l)}]}{\partial x_{k_{(l)}}} \right] = 0 \end{aligned}$$

for $n = 1, \dots, \infty$. (6)

The first tensor equation of this infinite chain propagates $R_{i_{(2)}}$ which has a close link to the Reynolds stress tensor, i.e.

$$\lim_{x_{(k)} \rightarrow x_{(l)}} R_{i_{(2)}} = \lim_{x_{(k)} \rightarrow x_{(l)}} R_{i_{(0)}i_{(1)}} = \overline{u_{i_{(0)}} u_{i_{(1)}}}(\mathbf{x}_{(l)}) \quad \text{mit } k \neq l, \quad (7)$$

These equations have to be completed by continuity equations and further permutation conditions, such as $R_{ij}(\mathbf{x}_{(0)}, \mathbf{x}_{(1)}) = R_{ji}(\mathbf{x}_{(1)}, \mathbf{x}_{(0)})$.

The two correlation equations (2) and (6) appear to have very different character as (2) is linear while (6) is nonlinear.

Further, in (2) coupling between equations appear only between equations of order n and $n + 1$. In contrast, in (6) all equations have a coupling to the second moment due to the last term in the third line and, additionally, each equation of order $n + 1$ has a coupling to equation of order n and $n + 2$.

Still, physics in both equations is fully equivalent and it is straight forward to employ the Reynolds decomposition $U_i = \bar{U}_i + u_i$ and $P = \bar{P} + p$ to derive relations between the classical $R_{i\{n+1}}$ and above $H_{i\{n+1}}$ definitions of correlations

$$H_{i(0)} = \bar{U}_{i(0)}, \quad (8)$$

$$H_{i(0)i(1)} = \bar{U}_{i(0)}\bar{U}_{i(1)} + R_{i(0)i(1)}, \quad (9)$$

$$H_{i(0)i(1)i(2)} = \bar{U}_{i(0)}\bar{U}_{i(1)}\bar{U}_{i(2)} + R_{i(0)i(1)}\bar{U}_{i(2)} + R_{i(0)i(2)}\bar{U}_{i(1)} + R_{i(1)i(2)}\bar{U}_{i(0)} + R_{i(0)i(1)i(2)} \quad (10)$$

where presently only the first three moments are given.

Lie Point Symmetries

Presently, any symmetry we are referring to is a Lie symmetry group which constitutes a transformation that maps equations to itself such as the scaling group $t^* = e^{2a}t$, $x^* = e^ax$, $T^* = T$ maps the heat equation $T_t = T_{xx}$ to itself i.e. $T_t^* = T_{x^*x^*}$. Apart from deep understanding of the underlying physics the key properties of Lie symmetries is that they form the basis for constructing invariant solutions, in fluid mechanics often referred to similarity solution if a scaling symmetry is involved. An elementary introduction to the theory of Lie symmetries is given in Hydon (2000).

Presently, Lie-point analysis allows us to derive special solutions, which, as will be seen later, verify known and new scaling laws of turbulent flows.

The first step is to find Lie-point symmetries of the given PDE, in our case of the MPC equations (2), which, at a later stage, will be reformulated into the $R_{i\{n}}$ formulation, which allows to reduce the two-point second moments to the Reynolds stresses. The symmetries to be searched for are transformations of the independent variables t , $\mathbf{x}_{(0)}$, $\mathbf{x}_{(1)}$, ... and the dependent functions $H_{i\{n}}$, $I_{i\{n-1}\{q}}$, where the transformed equations are equivalent to the MPC equations, i.e. form invariant under these transformations.

As expected, all symmetries of the Navier-Stokes equations transfer to the MPC equations (2), i.e. the Galilean group plus some scaling symmetries (see e.g. Rosteck, 2013). Here we will only give the two scaling groups needed below, which, in the limit of vanishing viscosity, read

$$T_{s1} : t^* = t, \mathbf{x}^* = e^{a_1}\mathbf{x}, \mathbf{r}_{(j)^*} = e^{a_1}\mathbf{r}_{(j)}, \quad (11)$$

$$H_{i\{n}}^* = e^{na_1}H_{i\{n}}, I_{i\{n}}^* = e^{(n+2)a_1}I_{i\{n}},$$

referring to scaling of space, while scaling of time reads

$$T_{s2} : t^* = e^{a_2}t, \mathbf{x}^* = \mathbf{x}, \mathbf{r}_{(j)^*} = \mathbf{r}_{(j)}, \quad (12)$$

$$H_{i\{n}}^* = e^{-na_2}H_{i\{n}}, I_{i\{n}}^* = e^{-(n+2)a_2}I_{i\{n}},$$

Most important, however, the system (1) admits additional symmetries, of purely statistical nature. They were first recognized in Oberlack & Rosteck (2010) and significantly extended in Rosteck (2013) and may be referred to as statistical symmetries.

The statistical symmetries for the **H-I**-system (2) can be separated into three distinct and generic sets of symmetries

$$\bar{T}'_1 : t^* = t, \mathbf{x}^* = \mathbf{x}, \mathbf{r}_{(l)}^* = \mathbf{r}_{(l)} + \mathbf{a}_{(l)}, \quad (13)$$

$$\mathbf{H}_{\{n}}^* = \mathbf{H}_{\{n}}, \mathbf{I}_{\{n}}^* = \mathbf{I}_{\{n}},$$

$$\bar{T}'_{2\{n}} : t^* = t, \mathbf{x}^* = \mathbf{x}, \mathbf{r}_{(l)}^* = \mathbf{r}_{(l)}, \quad (14)$$

$$\mathbf{H}_{\{n}}^* = \mathbf{H}_{\{n}} + \mathbf{C}_{\{n}}, \mathbf{I}_{\{n}}^* = \mathbf{I}_{\{n}} + \mathbf{D}_{\{n}},$$

$$\bar{T}'_s : t^* = t, \mathbf{x}^* = \mathbf{x}, \mathbf{r}_{(l)}^* = \mathbf{r}_{(l)}, \quad (15)$$

$$\mathbf{H}_{\{n}}^* = e^{k_s}\mathbf{H}_{\{n}}, \mathbf{I}_{\{n}}^* = e^{k_s}\mathbf{I}_{\{n}}.$$

In the specific case of turbulent parallel shear flows, where x_2 is the wall-normal coordinate, an additional set of symmetries is admitted (see Rosteck, 2013) given by

$$\bar{T}'_{z\{n}} : t^* = t, x_2^* = x_2, \mathbf{r}_{(l)}^* = \mathbf{r}_{(l)}, \quad (16)$$

$$\mathbf{H}_{\{n}}^* = \mathbf{H}_{\{n}} + \mathbf{A}_{\{n\}x_2}, \mathbf{I}_{\{n}}^* = \mathbf{I}_{\{n}}.$$

For the derivation of the symmetries (13), (14) and (15) it was crucial to use the form (2), while in the following we concentrate on two-point correlations and Reynolds stresses which are based on fluctuations u_i and p , where the Reynolds stress tensor $\overline{u_i u_j}(\mathbf{x})$ and the two-point correlation tensor $R_{ij}(\mathbf{x}, \mathbf{r}) = \overline{u_i(\mathbf{x})u_j(\mathbf{x} + \mathbf{r})}$ are connected by the relation

$$\overline{u_i u_j}(\mathbf{x}) = \lim_{\mathbf{r} \rightarrow 0} R_{ij}(\mathbf{x}, \mathbf{r}). \quad (17)$$

Using (8)-(10), the statistical symmetries (13)-(16) may be re-written for the one-point quantities \bar{U}_i and $\overline{u_i u_j}$. From (15) we find

$$\bar{T}'_s : t^* = t, \mathbf{x}^* = \mathbf{x}, \bar{U}_i^* = e^{a_s}\bar{U}_i, \quad (18)$$

$$\overline{u_i u_j}^* = e^{a_s} [\overline{u_i u_j} + (1 - e^{a_s})\bar{U}_i\bar{U}_j], \dots$$

where the first two of an infinite row of symmetries (14) are given by

$$\bar{T}'_{2\{1\}} : t^* = t, \mathbf{x}^* = \mathbf{x}, \bar{U}_i^* = \bar{U}_i + C_i, \quad (19)$$

$$\overline{u_i u_j}^* = \overline{u_i u_j} + \bar{U}_i\bar{U}_j - (\bar{U}_i + C_i)(\bar{U}_j + C_j), \dots$$

and

$$\bar{T}'_{2\{2\}} : t^* = t, \mathbf{x}^* = \mathbf{x}, \bar{U}_i^* = \bar{U}_i, \quad (20)$$

$$\overline{u_i u_j}^* = \overline{u_i u_j} + C_{ij}, \dots$$

where in the above groups a_s , C_i and C_{ij} are group parameter.

Finally, (16) may reformulated accordingly such that for the mean velocity it has the form

$$\bar{T}'_{z\{1\}} : x_2^* = x_2, \bar{U}_1^* = \bar{U}_1 + b_1 x_2, \overline{u_i u_j}^* = \overline{u_i u_j}, \dots \quad (21)$$

while for the stresses we similarly obtain

$$\bar{T}'_{z\{2\}} : x_2^* = x_2, \bar{U}_1^* = \bar{U}_1, \overline{u_i u_j}^* = \overline{u_i u_j} + b_{ij} x_2, \dots \quad (22)$$

The above statistical groups (18)-(22) play an important role when calculating scaling laws for higher order moments Oberlack & Rosteck (2010); Rosteck (2013). In particular in Rosteck (2013) it was shown that (22) plays an important role for the second moments scaling laws for various shear flow, including the present ones, as may be taken from results below. However, in a companion paper Avsarkisov *et al.* (2015) of this conference the corresponding symmetry (21) for the mean velocity was substantiated the first time in DNS data of a turbulent Couette flow.

Group invariant solutions

From the set of all symmetries given above we may now construct invariant solutions which may be interpreted as turbulent scaling laws. For this it is important to note that group invariant solutions may only be properly constructed from the infinitesimal form of the groups (18)-(22) (see e.g. Hydon, 2000). Further, we should note that infinitesimals form a linear vector space and hence may be combined linearly. Without giving details of its derivation we present the invariant surface condition

$$\frac{dx_2}{a_1 x_2 + a_4} = \frac{d\bar{U}_1}{(a_1 - a_2 + a_s)\bar{U}_1 + C_1} = \frac{dR_{11}}{\xi_{R_{11}}} = \dots, \quad (23)$$

where its integration defines the invariant solutions for the mean velocity and higher moments. Different to the turbulent Couette flow which is investigated in Avsarkisov *et al.* (2015) we may presently skip the symmetry (21) as this appears to be special for the Couette flow and has not been observed in any other turbulent shear flow yet.

Turbulent scaling laws

Before we detail on turbulent wall-bounded shear flows, which is the primary focus of the present contribution, we may briefly mention decay of isotropic turbulence. For this type of a flow various different classes of scaling laws have been derived Oberlack & Rosteck (2010), Rosteck (2013) and Oberlack & Zieleniewicz (2013).

First of all, classical solution may be reproduced, where the kinetic energy decays algebraically with $k \sim (t + t_0)^{-m}$ and the integral length scale growth according to $\ell_t \sim (t + t_0)^n$. For this, however, it is important to note that due to the additional scaling group (15) values for m and n may not intimately connected as predicted by Birkhoff or Loitsianskii integrals and its generalizations.

Moreover, two different exponential scaling laws exist, where in both cases the turbulent kinetic energy decays as $k \sim e^{-at}$. The first case refers to a constant integral length scale $\ell_t \sim const.$ and appears to describe decaying turbulence generated by a fractal grid. The second has an increasing integral length scale according to an exponential function $\ell_t \sim e^{bt}$. This type of behavior has not been observed before and most likely is induced by a forcing of Navier-Stokes equations according to $-U/\tau$, where τ is a constant time scale.

Below we will primarily focus on wall-bounded shear flows and for this we will start with the most well-known of all scaling laws i.e. the logarithmic law of the wall. For this the scaling of space (11) and time (12) with the group parameter a_1 and a_2 as well as the statistical scaling symmetry (18) with the group parameter a_s are essential. We combine the three groups to a three-parameter group of the form

$$\bar{T}'_{s1,s2,s}: x_2^* = e^{a_1} x_2, \quad \bar{U}_1^* = e^{a_1 - a_2 + a_s} \bar{U}_1, \quad \dots \quad (24)$$

As the key dimensional parameter for the logarithmic law of the wall, the friction velocity $u_\tau = \sqrt{\tau_{wall}/\rho}$, has the dimen-

sion of a velocity, this may be considered a symmetry breaking quantity. For the three-parameter group (24) this means that scaling of the velocity is suppressed, which results in the constraint

$$a_1 - a_2 + a_s = 0. \quad (25)$$

Using the latter in the condition for invariant solution (23) it is apparent that the two terms on the left combine to logarithmic function. Introducing the classical +-variables we obtain the log-law in dimensionless form

$$u^+ = \frac{1}{\kappa} \ln(x_2^+ + A^+) + C, \quad (26)$$

where x_2^+ is the wall-normal direction. In a similar fashion, the Reynolds stresses can be derived from the two-point correlations, so that we finally gain

$$\overline{u_i u_j} = \frac{D_{ij}}{x_2^+ + A^+} + B_{ij}, \quad ij \neq 11 \quad (27)$$

$$\begin{aligned} \overline{u_1 u_1} &= \frac{D_{11}}{x_2^+ + A^+} - \frac{1}{\kappa^2} \ln^2(x_2^+ + A^+) \\ &\quad - 2 \frac{C}{\kappa} \ln(x_2^+ + A^+) + B_{11}. \end{aligned} \quad (28)$$

Therein, κ , A^+ , C , γ , D_{ij} and B_{ij} are constants.

As mentioned above, (26) and (28) is validated against the data of Jimenez & Hoyas (2008); Hoyas & Jimenez (2008). In Figure 1 scaling of (26) in the range $55 \leq x_2^+ \leq 325$ is considered, where parameters have been adjusted to $\kappa = 0.405$ and $C = 5.07$. In the region where the log-law (26) has its validity we also plot the Reynolds stress tensor (27) and (28) depicted in Figure 2 and in Figure 3.

In the 11-component, the leading order term in formula (28) is the logarithm squared with the factor $1/\kappa^2$. It is important to note that exactly this term is fixed through the parameter κ determined by the mean velocity. If κ would be smaller, we would not be able to fit the 11-component to the DNS data.

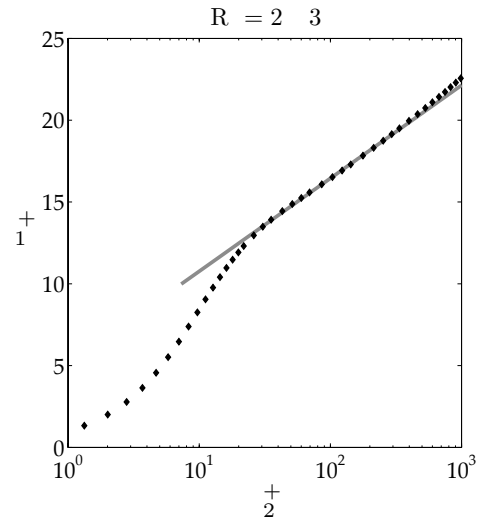


Figure 1. DNS data of Jimenez & Hoyas (2008); Hoyas & Jimenez (2008) are compared to the scaling law (26).

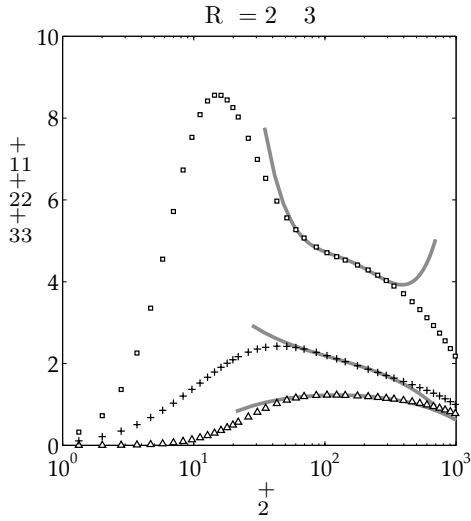


Figure 2. DNS data of Jimenez & Hoyas (2008); Hoyas & Jiménez (2008) for the stresses $\overline{u_1 u_1^+}$ (\square), $\overline{u_2 u_2^+}$ (\triangle) and $\overline{u_3 u_3^+}$ ($+$) are compared to the scaling laws (27) (solid lines).

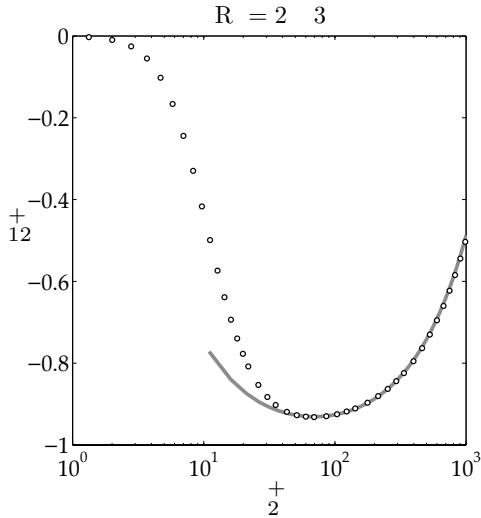


Figure 3. DNS data of Jimenez & Hoyas (2008); Hoyas & Jiménez (2008) for the stresses $\overline{u_1 u_2^+}$ is compared to the scaling laws (27) (solid lines).

The method of Lie symmetries is not restricted to simple shear flows and subsequently we consider rotating turbulent channel flows, for which different scaling laws are calculated depending on the direction of the rotational axis (details may be taken from the PhD thesis by Rosteck 2013).

Though results are apparently not limited to the mean velocity, the actual results for the stresses and higher order moments may be extremely involved, and, hence, we presently limit formulas to the mean velocity, while details for higher moments may be taken from Rosteck (2013).

In the first test case we consider a pressure-driven turbulent channel flow. For the center region of the flow it was already presumed in Oberlack (2001), that we attain a maximum degree of symmetry and, hence, integration of the two far most terms on the left of the invariant surface condition (23) yields a power law. Reformulating in dimensional variables we obtain

$$\bar{U}^{def+} = \frac{U_{cl} - \bar{U}(x_2)}{u_\tau} = \beta \left(\frac{x_2}{h} \right)^\alpha, \quad (29)$$

which is compared to the DNS data of Jimenez & Hoyas (2008); Hoyas & Jiménez (2008) in Figure 4.

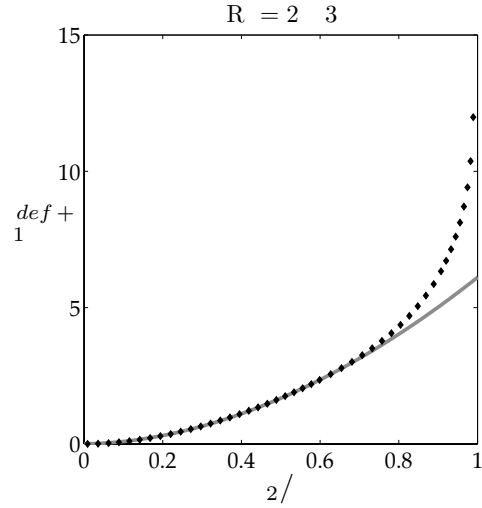


Figure 4. DNS data of Jimenez & Hoyas (2008); Hoyas & Jiménez (2008) are compared to the scaling law (29).

Correspondingly, stresses for this region are compared in Figure 5.

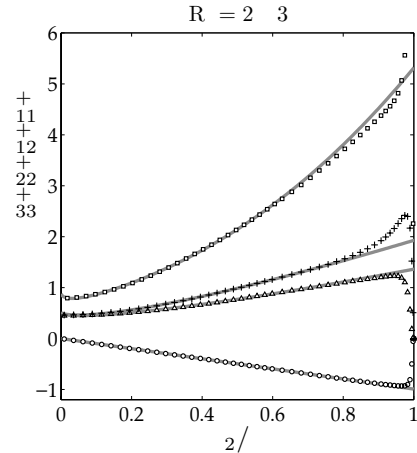


Figure 5. Comparison of the Reynolds stress scaling law (—) (formula omitted) with the DNS data of Jimenez & Hoyas (2008); Hoyas & Jiménez (2008).

The following two test cases are variations of the previously considered Poiseuille flow imposing system rotation.

In the first test case we assume span-wise rotation, i.e. the axis of rotation is parallel to x_3 , i.e. only Ω_3 is non-zero. Here, a first attempt to analyze this flow applying Lie symmetry analysis was published in Oberlack (2001) giving a linear mean velocity with its gradient is proportional to the rotational speed.

The more recent analysis Rosteck (2013) showed that the linear behavior is only true in the limit of large Ω_3 and, in fact, an exponential behavior appears to be the correct solution to this

problem

$$\frac{\bar{U}_1(x_2) - \bar{U}_{cl}}{\Omega_3 h} = A(Ro_2) \left(e^{\gamma(Ro_3) x_2/h} - 1 \right), \quad (30)$$

where $A(Ro_3)$ and $\gamma(Ro_3)$ are unknown functions of the rotation number $Ro_3 = \frac{2\Omega_3 h}{U_b}$, though its functional form has not been determined from symmetry theory yet. U_b and \bar{U}_{cl} are respectively bulk and center line velocity. $\gamma(Ro_3)$ converges to zero for increasing Ro_3 , while $A(Ro_3)$ tends to a constant in this limit. Carrying out the latter limit $Ro_3 \rightarrow \infty$ we obtain the well-known scaling law for a rotating channel about the x_3 -axis (see Oberlack, 2001)

$$\bar{U}_1(x_2) = A_\infty \Omega_3 x_2 + \bar{U}_{cl}. \quad (31)$$

A clear validation of (30) and (31) is given in Figure 6 for various Ω_3 taken from the DNS of Kristoffersen & Andersson (1993). Interesting enough the value for A_∞ appears to approach the value 2, which corresponds to a zero mean vorticity in an absolute from of reference.

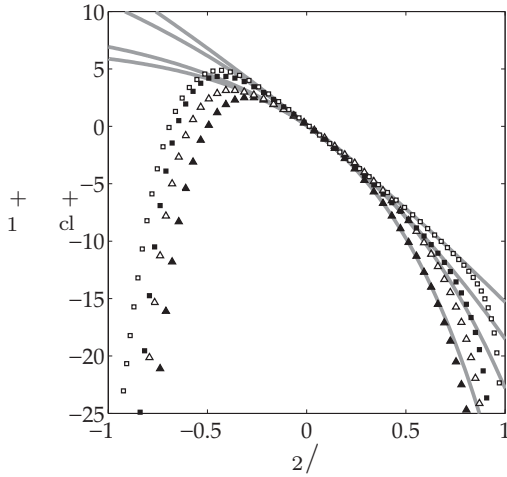


Figure 6. Comparison of the mean velocity scaling law (—) in (30) with the DNS data (···) of Kristoffersen & Andersson (1993) at various rotation rates $Ro_3 = \frac{\Omega_3 h}{u_\tau}$ and $Re_\tau = 194$.

In respect to the stresses the DNS data of Kristoffersen & Andersson (1993) only provide the kinetic energy, which are compared to the scaling law in Figure 7.

In the next test case we assume wall-normal rotation i.e. rotation about the x_2 -axis and, due to the Coriolis induced cross flow in x_3 -direction, two velocity components \bar{U}_1 and \bar{U}_3 have to be taken into consideration. Again, both averaged velocities may only depend on x_2 . Rewriting the underlying symmetries in a rotating frame the resulting scaling laws is of the form:

$$\begin{aligned} \bar{U}_1 &= \left(\frac{x_2}{h}\right)^b \left[a_1 \cos\left(cRo_2 \cdot \ln \frac{x_2}{h}\right) \right. \\ &\quad \left. + a_2 \sin\left(cRo_2 \cdot \ln \frac{x_2}{h}\right) \right] + d_1(Ro_2) \\ \bar{U}_3 &= \left(\frac{x_2}{h}\right)^b \left[a_1 \sin\left(cRo_2 \cdot \ln \frac{x_2}{h}\right) \right. \end{aligned}$$

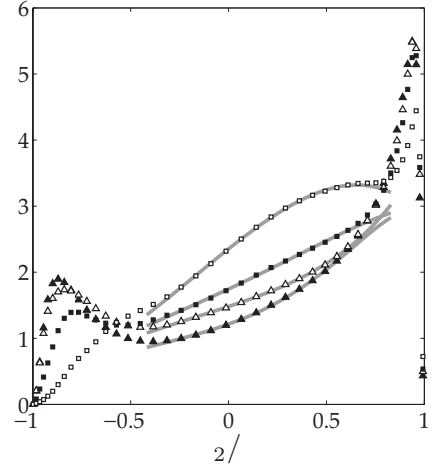


Figure 7. Comparison of the turbulent kinetic scaling law (—) (formula omitted) with the DNS data (···) of Kristoffersen & Andersson (1993) at various rotation rates $Ro_3 = \frac{\Omega_3 h}{u_\tau}$ at $Re_\tau = 194$.

$$-a_2 \cos\left(cRo_2 \cdot \ln \frac{x_2}{h}\right) + d_2(Ro_2). \quad (32)$$

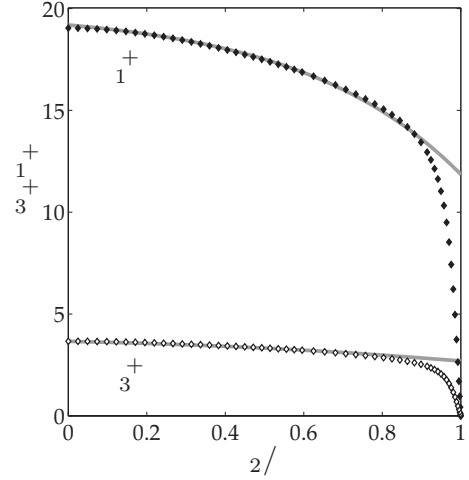


Figure 8. Comparison of the mean flow scaling law (—) in (32) with the DNS data (···) of Mehdizadeh & Oberlack (2010) at $Re_\tau = 360$ and $Ro_2 = 0.011$.

The latter is compared to the DNS data of Mehdizadeh & Oberlack (2010) at $Re_\tau = 360$. Results are depicted for three different rotation numbers $Ro_2 = \frac{2\Omega_2 h}{u_{\tau 0}}$ in the Figures 8, 9 and 10 exhibiting an excellent fit in the center of the channel for all cases. Here, $u_{\tau 0}$ refers to the friction velocity of the non-rotating case. It is to note that from the DNS data in Mehdizadeh & Oberlack (2010) we find that with an increasing Ω_2 the magnitude of \bar{U}_1 and \bar{U}_3 switch positions since with increasing rotation rates \bar{U}_1 is suppressed while \bar{U}_3 increases up to a certain point and decreases again though to a smaller extent compared to \bar{U}_1 . This behavior is exactly described by the scaling law (32).

From the previous three cases we have singled out the case with $Ro_2 = 0.072$ to present the stresses shown in Figure 11.

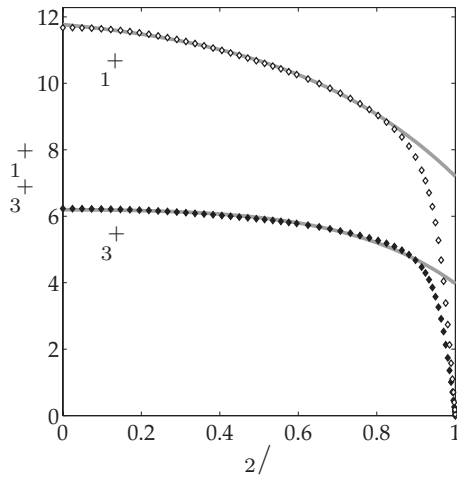


Figure 9. Comparison of the mean flow scaling law (—) in (32) with the DNS data (···) of Mehdizadeh & Oberlack (2010) at $Re_\tau = 360$ and $Ro_2 = 0.072$.

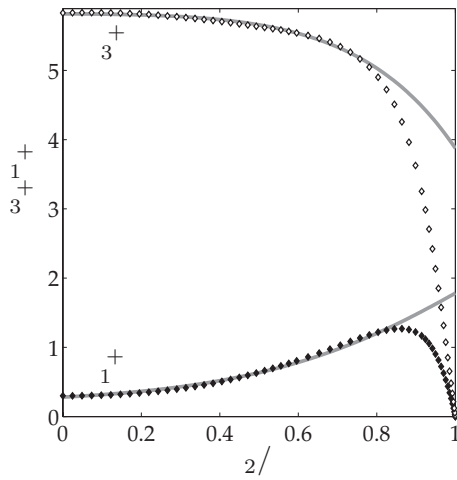


Figure 10. Comparison of the mean flow scaling law (—) in (32) with the DNS data (···) of Mehdizadeh & Oberlack (2010) at $Re_\tau = 360$ and $Ro_2 = 0.18$.

Conclusion

The key results of present abstract ist that the symmetry based turbulence theory in Oberlack (2001) has been considerable extended to be application higher order multi-point correlations. Presently, we applied it to several canonical flows such as decaying turbulence and wall-bounded turbulent shear flows including frame rotating and wall-transpiration and we have explicitly computed scaling laws for both mean velocity and second moments.

REFERENCES

- Avsarkisov, V., Oberlack, M., Hoyas, S., Rosteck, A., Garcia-Galache, J.-P. & Frank, A. 2015 Plane turbulent couette flow: Dns, large scale structures and symmetry induced scaling laws. Proceedings of the 9th Symposium on Turbulence and Shear Flow Phenomena, Melbourne, Australia.
- Hoyas, S. & Jiménez, J. 2008 Reynolds number effects on the reynolds-stress budgets in turbulent channels. *Physics of Fluids* **20** (10), 101511.
- Hydon, P.E. 2000 *Symmetry Methods for Differential Equations. A Begimmer's Guide.*. Cambridge University Press, UK.

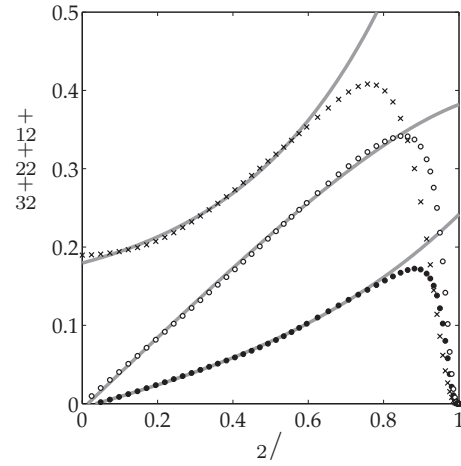


Figure 11. Comparison of the Reynolds stress scaling law (—) (formula omitted) with the DNS data (···) of Mehdizadeh & Oberlack (2010) at $Re_\tau = 360$ and $Ro_2 = 0.072$.

- Jimenez, J. & Hoyas, S. 2008 Turbulent fluctuations above the buffer layer of wall-bounded flows. *J. Fluid Mech.* **611**, 215–236.
- Keller, L. & Friedmann, A. 1925 Differentialgleichungen für die turbulente bewegung einer kompressiblen flüssigkeit. pp. 395–405. Proceedings of the First International Congress for Applied Mechanics, Technische Boekhandel en Drukkerij J. Waltman Jr., Delft, Netherlands.
- Kristoffersen, R. & Andersson, H.I. 1993 Direct simulations of low-reynolds-number turbulent flow in a rotating channel. *J. Fluid Mech.s* **256**, 163–197.
- Mehdizadeh, A. & Oberlack, M. 2010 Analytical and numerical investigations of laminar and turbulent poiseuille ekman flow at different rotation rates. *Phys. of Fluids* **22**, 105104.
- Oberlack, M. 2001 A unified approach for symmetries in plane parallel turbulent shear flows. *J. Fluid Mech.* **427**, 299–328.
- Oberlack, M. & Rosteck, A. 2010 New statistical symmetries of the multi-point equations and its importance for turbulent scaling laws. *Discrete Contin. Dyn. Sys., Ser. S* **3**, 451–471.
- Oberlack, M. & Zieloniewicz, A. 2013 Statistical symmetries and its impact on new decay modes and integral invariants of decaying turbulence. *Journal of Turbulence* **14**(2), 4–22.
- Rosteck, A. 2013 Scaling laws in turbulence - a theoretical approach using lie-point symmetries. *Doctoral thesis, TU Darmstadt*.